Temporal contrast sensitivity in the lateral geniculate nucleus of a New World monkey, the marmoset *Callithrix jacchus*

Samuel G. Solomon, Andrew J. R. White and Paul R. Martin

Department of Physiology and Institute for Biomedical Research, University of Sydney, NSW 2006, Australia

(Received 19 November 1998; accepted after revision 3 March 1999)

1. The temporal contrast sensitivity of koniocellular, parvocellular and magnocellular cells in the lateral geniculate nucleus (LGN) of nine adult marmosets was measured. The receptive fields of the cells were between 0·3 and 70 deg from the fovea. The stimulus was a large spatially uniform field which was modulated in luminance at temporal frequencies between 0·98 and 64 Hz.

2. For each cell group there was a gradual increase in modulation sensitivity, especially for temporal frequencies below 8 Hz, with increasing distance from the fovea. At any given eccentricity, magnocellular cells had the greatest sensitivity. In central visual field, the sensitivity of koniocellular cells lay between that of parvocellular and magnocellular cells. In peripheral visual field (above 10 deg eccentricity) koniocellular and parvocellular cells had similar sensitivity.

3. The contrast sensitivity of each cell class was dependent on the anaesthetic used. Cells from animals anaesthetized with isoflurane were less sensitive than cells from animals anaesthetized with sufentanil. This effect was more marked for temporal frequencies below 4 Hz.

4. These results are incompatible with the notion that the koniocellular pathway is functionally homologous to a sluggish, W-like pathway in other mammals. At least in terms of their temporal transfer properties, many koniocellular cells are more like parvocellular cells.

The temporal response properties of cells in the two main subdivisions of the primate retinocortical pathway are well established. Parasol ganglion cells and their recipient cells in the magnocellular layers of the lateral geniculate nucleus (LGN) differ from those in the midget-parvocellular pathway in several ways. They respond to higher temporal frequencies, have greater sensitivity to achromatic contrast, and their temporal modulation transfer function for achromatic contrast shows more bandpass characteristics (De Monasterio & Gouras, 1975; Derrington & Lennie, 1984; Kaplan & Shapley, 1986; Lee *et al.* 1990; Yeh *et al.* 1995; Kremers *et al.* 1997). The properties of cells in the more recently recognized third geniculocortical pathway, the koniocellular/interlaminar pathway, are less well understood. In the nocturnal prosimian *Galago* (Norton & Casagrande, 1982; Irvin *et al.* 1986, 1993; Norton *et al.* 1988) and in the tree shrew *Tupaia* (Holdefer & Norton, 1995), the koniocellular/interlaminar pathway includes cells with a variety of spatial characteristics. Many of the koniocellular cells in *Galago* have spatial properties intermediate between those of parvocellular and magnocellular cells (Norton *et al.* 1988; Casagrande & Norton, 1991), and the spatial action spectrum of koniocellular cells can account for at least part of the behavioural contrast sensitivity function in that species (Bonds *et al.* 1987; Norton *et al.* 1988). A sample of koniocellular/interlaminar pathway cells in *Galago* showed sluggish, relatively phasic responses to square-wave temporal modulation (Irvin *et al.* 1986) but the temporal transfer properties in the koniocellular pathway have not been studied systematically in any simian primate.

The retinogeniculate pathway of diurnal New World monkeys such as the marmoset *Callithrix jacchus* shares many functional and structural features with that of Old World primates such as macaques (Troilo *et al.* 1993; Yeh *et al.* 1995; Kremers & Weiss, 1997; Kremers *et al.* 1997; White *et al.* 1998). The marmoset has a fovea which is quantitatively similar to that of macaque (Walls, 1953; Wilder *et al.* 1996). In the marmoset LGN there is a well segregated koniocellular division between the parvocellular and magnocellular layers (Kaas *et al.* 1978; Goodchild & Martin, 1998). This makes it possible to localize accurately physiological recordings to cells in this region (Martin *et al.* 1997). The sensitivity to achromatic contrast of parvocellular and magnocellular cells in marmoset LGN is similar to their counterparts in macaque LGN (Yeh *et al.* 1995; Kremers & Weiss, 1997; Kremers *et al.* 1997). In the present study we extend these observations to koniocellular cells and compare cells from all these groups for a wide range of visual field

positions. We show that the temporal contrast sensitivity of koniocellular cells is close to that of parvocellular cells, and that the sensitivity of all pathways to low frequency temporal modulation increases as a function of retinal eccentricity. Some of these results have appeared elsewhere in abstract form (Solomon *et al.* 1998).

METHODS

Animal preparation

Recordings were made from nine adult marmosets (*Callithrix jacchus*) of body weight 250–370 g. Animals were obtained from the Australian National Health and Medical Research Council (NHMRC) combined breeding facility in Adelaide. Three of the animals were male, the others were female. All procedures used conform with the provisions of the Australian NHMRC code of practice for the care and use of animals. All animals were initially sedated with isoflurane (ICI, 1·5–2%) and anaesthetized with intramuscular ketamine (30 mg kg^{-1}) for surgery. A femoral vein and the trachea were cannulated. Animals were artificially respired with a 70%–30% mixture of NO_2 : Carbogen (5% CO_2 in O_2). A venous infusion of 40 μg kg^{-1} h^{-1} alcuronium chloride (Alloferin, Roche) in dextrose Ringer solution was infused at a rate of 1 ml h^{-1} to maintain muscular relaxation. In some experiments, anaesthesia was maintained during recording with isoflurane (0·25–0·75%) and in others by intravenous infusion of sufentanil citrate (Sufenta-Forte, Janssen-Cilag, Beerse, Belgium; 4–8 μg kg^{-1} h^{-1}). Electroencephalogram and electrocardiogram signals were monitored to ensure adequate depth of anaesthesia. End-tidal CO_2 was measured and maintained near 4% by adjusting the rate and stroke volume of the inspired gas mixture. The pupils were dilated with topical neosynephrine. Penicillin and corticosteroids were administered daily.

The animal was mounted in a stereotaxic head-holder. The eyes were protected with oxygen-permeable contact lenses and focused on a tangent screen at a distance of 114 cm. The stereotaxic frame was tilted to bring the optical axis close to the horizontal plane, and the positions of the fovea and optical disk were mapped onto the tangent screen with the aid of a fundus camera equipped with a rear projection device. The table supporting the stereotaxic frame could be rotated as required to bring the receptive fields of recorded cells close to the centre of the tangent screen. Such movements were monitored by means of a laser attached to the table.

A craniotomy was made over the LGN and a microelectrode (parylene-coated tungsten or glass-coated steel; impedance 5–12 MΩ, F. H. Haere Co., Bowdoinham, ME, USA) was lowered into the LGN. Action potentials arising from visually responsive units were identified (Bishop *et al.* 1962). The time of their occurrence was measured with an accuracy of 0·1 ms and recorded.

Visual stimuli

Each visually responsive cell was initially classified using hand-held stimuli; thereafter all stimuli were delivered through a Maxwellian view system (Smith *et al.* 1992; Yeh *et al.* 1995) which was aligned along the axis of the receptive field of the cell, and centred on the pupil of the eye. The stimulus in the plane of the pupil was a spatially uniform field composed of the combined image of red and green light-emitting diodes (LEDs) with dominant wavelengths of 639 and 554 nm. Time-averaged illuminance measured according to Westheimer (1966), using a PR-650 spectrophotometer (Photo Research, Chatsworth, CA, USA), for the red and green LEDs combined, was close to 1000 photopic trolands (td). The smaller size of the marmoset eye (Troilo *et al.* 1993) means that retinal flux per troland is almost four times higher than for humans. An 8 or 2 mm aperture was placed at the rear focal plane of the Maxwellian view lens to give a stimulus subtense of 6·4 or 1·6 deg. The stimuli were usually unattenuated to minimize the possibility of rod intrusion (Kremers *et al.* 1997). For some cells (usually off-centre), responses were enhanced by attenuation with a 1 neutral density (ND) filter, so this was used.

The red and green diodes were modulated in phase. Contrast was varied with a sine envelope over 8·192 s (for 0·98 Hz modulation frequency) or 4·096 s (for other modulation frequencies). These rather strange-looking numbers were chosen to allow integer multiples of the contrast modulation period in a constant envelope: for example, 16 cycles at 3·91 Hz (period 256 ms) gives 4·096 s. Each cell encountered was tested first with a temporal frequency of 3·91 Hz. A series of sequentially higher temporal frequencies was then tested. At least one measurement was made at a frequency higher than the point where a modulated response disappeared, as judged by auditory monitoring of the spike discharge. Lower frequencies were tested to the limit (0·98 Hz) imposed by the signal generation software. The maximum contrast of the stimulus was reduced to 50, 25 or 12·5% as required for cells showing high contrast sensitivity, so as to increase the sampling density in the low contrast range.

Histological processing

The position of each recorded cell was noted by reading the depth from the hydraulic microelectrode advance (David Kopf Model 640). Electrolytic lesions (6–20 μA for 10–20 s, electrode negative) were made to mark the location of electrode tracks. At the end of the recording session the animal was killed with an overdose of pentobarbitone sodium (80–150 mg kg^{-1}, I.V.) and perfused with 0·25 l of saline (0·9% NaCl) followed by 0·3 l of freshly prepared 4% paraformaldehyde in 0·1 M phosphate buffer (PB, pH 7·4). The brain was removed and postfixed in the 4% paraformaldehyde in PB for 6 h then placed in 30% sucrose in PB until it sank. Coronal sections at 30 μm thickness were cut on a freezing microtome; the sections were mounted onto glass slides, air dried, then stained with Cresyl Violet. The position of recorded cells was reconstructed by identifying the electrolytic lesions and correlating changes in eye allegiance with the laminar pattern revealed by the Cresyl Violet stain.

RESULTS

We quantified the responses of 130 cells in the LGN. Our criteria for accepting cells for analysis were that the maximum first harmonic of response to 3·91 Hz modulation exceeded 10 impulses s^{-1} and that the position of the recorded cell could be assigned to the parvocellular, koniocellular or magnocellular division of the LGN. Of these cells, 80 were located to the parvocellular layers, 15 to the magnocellular layers, 30 to the koniocellular layer between the internal magnocellular and parvocellular layers and 5 to the S layer lying below the external magnocellular layer (see Fig. 1). We have estimated previously that the uncertainty in cell position introduced by the histological reconstruction process means that any given cell should lie within a 75 μm radius of its nominal position (Martin *et al.* 1997). This means that a small fraction of cells will inevitably be

assigned to the incorrect subdivision of the LGN, but we have no reason to believe that there would be a bias towards any (parvocellular, koniocellular or magnocellular) division of the LGN.

Two of the female marmosets were trichromatic, as judged by analysis of responses to a red–green phase-varying stimulus described elsewhere (Yeh *et al.* 1995; White *et al.* 1998). One of these animals gave responses consistent with the presence of cones with peak sensitivities near 556 nm and 563 nm; the other animal was consistent with a 543 nm/563 nm phenotype. The remaining three females and the three males were dichromats. For the present analysis we only included cells that showed no sign of red–green opponent interactions.

The amplitude and phase of cell response at each temporal frequency were measured by Fourier analysis of spike density as shown in Fig. 2 for an off-centre parvocellular cell. The response was analysed by dividing the stimulus epoch into 'slices', each of which corresponds to one cycle of contrast modulation (Fig. 2*A*, *B* and *C*). The first harmonic amplitude was used for analysis of contrast sensitivity. For this cell the first harmonic amplitude corresponds well to the average impulse density (Fig. 2*C*), with some distortion apparent at high contrast levels.

We fitted a Naka–Rushton function to the amplitude data. Its form is:

$$R(C) = R_{\mathrm{m}}C/(b + C),$$

where C is contrast, R_{m} is the maximum response amplitude and b is the contrast eliciting half the maximal response (Naka & Rushton, 1966). Although this function clearly cannot account for all aspects of the responses seen in the large numbers of cells tested, we found it gave the best overall account of contrast–response relationships with the minimum number of free parameters. We fixed the response to pass through zero at zero contrast. Adding a third free parameter to translate the contrast–response function on either the X axis ('contrast threshold') or Y axis ('spontaneous activity') produced insignificant improvement in the residual error values for each curve (data not shown). At the high illuminance level of the stimulus the spontaneous response rate was low for the majority of cells tested. We measured the power at each stimulus frequency for an unmodulated stimulus for a sample of cells ($n = 10$); the spontaneous activity was less than 2 impulses s^{-1} for all cells.

The continuous slow variation in stimulus contrast due to the sine envelope meant that the stimulus sign was opposite for equivalent slices in the rising and falling phases of the

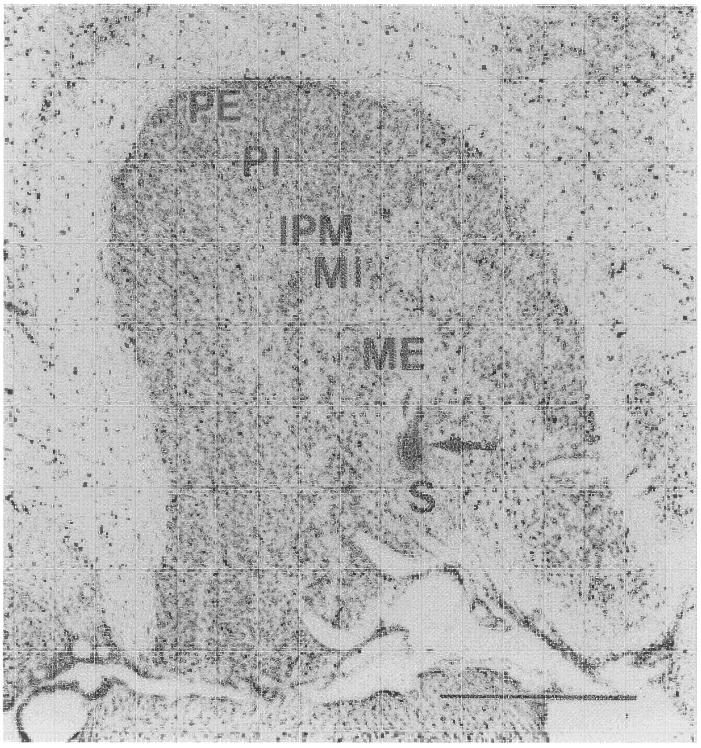

Figure 1. Nissl-stained coronal section (30 μm thickness) through the LGN of the marmoset

The section shows the dorsal parvocellular layers, the ventral magnocellular layers and the koniocellular layers, which lie between the internal parvocellular and magnocellular layers, and ventral to the magnocellular layers. An electrolytic lesion used to reconstruct the electrode track is indicated by the arrow. Scale bar, 1 mm. Abbreviations according to Kaas *et al.* (1978): PE, external parvocellular layer; PI, internal parvocellular layer; IPM, interlaminar (koniocellular) layer; MI, internal magnocellular layer; ME, external magnocellular layer; S, superficial (koniocellular) layer.

stimulus epoch. Most cells (such as the one shown in Fig. 2) showed some rectification of their response. The upshot of this is that the response amplitude of on-centre cells is slightly greater in the falling phase of the epoch, and the response amplitude of off-centre cells is slightly greater in the rising phase. For curve fitting we averaged the responses to rising and falling phases. Figure 2*D* shows fits obtained from the rising and falling phases for the cell response shown in Fig. 2*A*, as well as a fit derived from the average of the two phases. The effect of the response asymmetry on contrast gain estimates is discussed further below.

Examples of responses from cells within each LGN subdivision are shown in Fig. 3. Responses of magnocellular

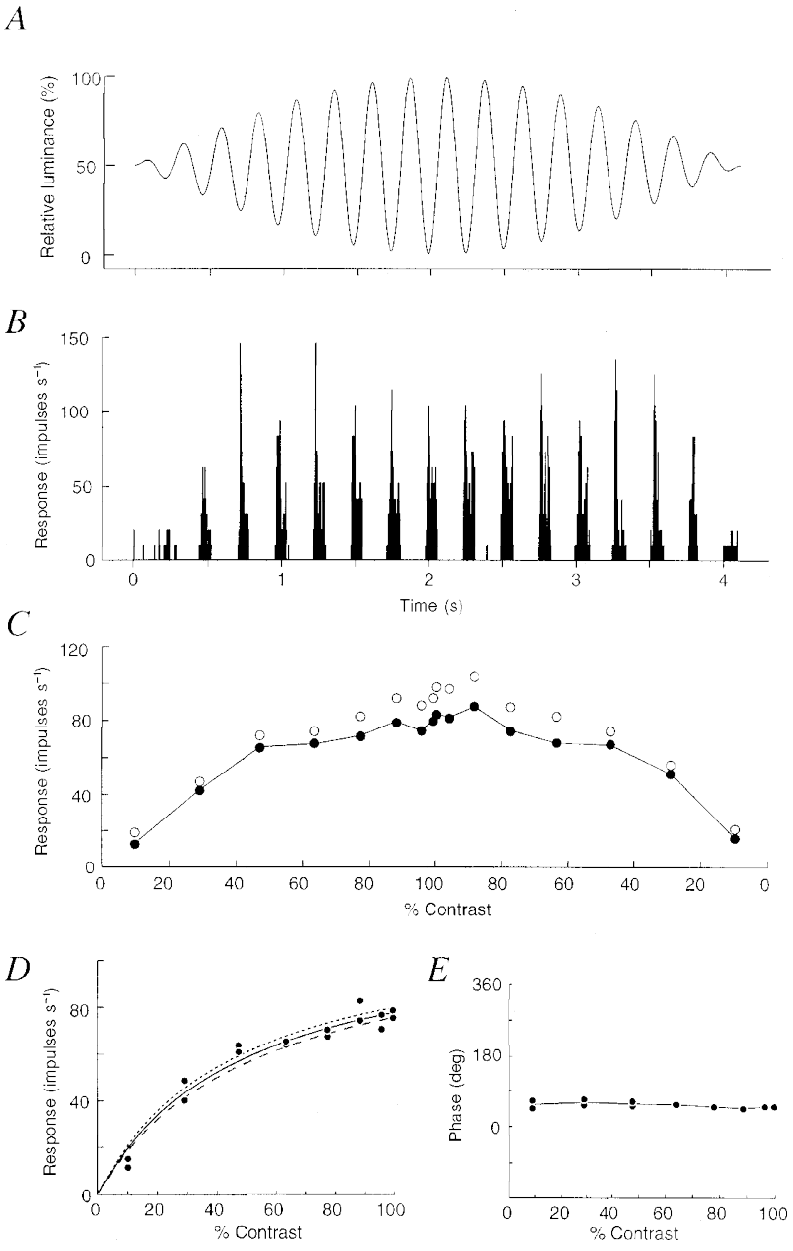

Figure 2. Response of an off-centre parvocellular cell

A, sketch of the stimulus waveform. The contrast modulation frequency is 3·91 Hz. The contrast varies with a sine envelope over 4·096 s. *B*, peristimulus time histogram (PSTH) of cell response. Mean of 24 stimulus presentations. *C*, amplitude of the first harmonic (●) and zero order harmonic (mean spike frequency, ○) of the 3·91 Hz Fourier component of the PSTH. *D*, Naka–Rushton function fitted to the first harmonic amplitude obtained from (1) both the rising and falling phases of the stimulus epoch (continuous line), (2) the rising phase only (dashed line) or (3) the falling phase only (dotted line). The initial slope of the fitted function was 2·18 impulses s^{-1} (% contrast)$^{-1}$ for the rising phase, 2·55 impulses s^{-1} (% contrast)$^{-1}$ for the falling phase and 2·36 impulses s^{-1} (% contrast)$^{-1}$ when both phases were used. *E*, phase of first harmonic of response shown in *C* and *D*.

and parvocellular cells were consistent with previous reports on marmoset (Yeh *et al.* 1995; Kremers *et al.* 1997) and macaque (Derrington & Lennie, 1984; Kaplan & Shapley, 1986; Lee *et al.* 1990). The magnocellular cell (Fig. 3*B*) responds to low contrast levels and shows significant response saturation at all stimulus frequencies for higher contrasts. The parvocellular cell (Fig. 3*A*) has lower contrast sensitivity and shows little sign of response saturation at any frequency. A range of response patterns was seen in koniocellular cells. Two examples are shown in Fig. 3*C* and *D*. These cells had overlapping receptive field locations and were recorded in the same electrode track within 50 μm of each other. One cell (Fig. 3*C*) shows no response saturation at any temporal frequency and does not respond to modulation above 10 Hz; the other (Fig. 3*D*) shows considerable response saturation at moderate frequencies and has a higher cut-off frequency.

Contrast sensitivity and receptive field eccentricity

For each cell the contrast gain (impulses s^{-1} (% contrast)$^{-1}$) for 3·91 Hz modulation was calculated from the initial slope of the Naka–Rushton function, R_m/b (Lee *et al.* 1990; Croner & Kaplan, 1995; Kremers *et al.* 1997). We found no systematic difference in contrast sensitivity between dichromats and trichromats for any cell group (Fig. 4*A*). In agreement with Kremers *et al.* (1997) we also found no consistent difference in the responses to 1·6 or 6·4 deg field. Responses in the cells where the stimulus was attenuated with a 1 ND filter were consistent with those of cells where the stimulus was unattenuated, so we grouped all available data.

The sensitivity of parvocellular cells increases with eccentricity (Fig. 4*B*). A regression line fitted to the gain of parvocellular cells shows significant slope (gain = $0{\cdot}263 \times \mathrm{Ecc}^{0{\cdot}39}$, $P < 0{\cdot}001$, $n = 77$), where Ecc is eccentricity, but weak correlation ($r^2 = 0{\cdot}18$). The gain of the other two cell classes shows a non-significant increase with eccentricity (magnocellular: gain = $0{\cdot}912 \times \mathrm{Ecc}^{0{\cdot}44}$, $r^2 = 0{\cdot}21$, $P = 0{\cdot}09$, $n = 15$; koniocellular: gain = $0{\cdot}437 \times \mathrm{Ecc}^{0{\cdot}21}$, $r^2 = 0{\cdot}02$, $P = 0{\cdot}4$, $n = 35$). Overall, the sensitivity of koniocellular cells falls between that of the magnocellular and parvocellular groups at 3·91 Hz.

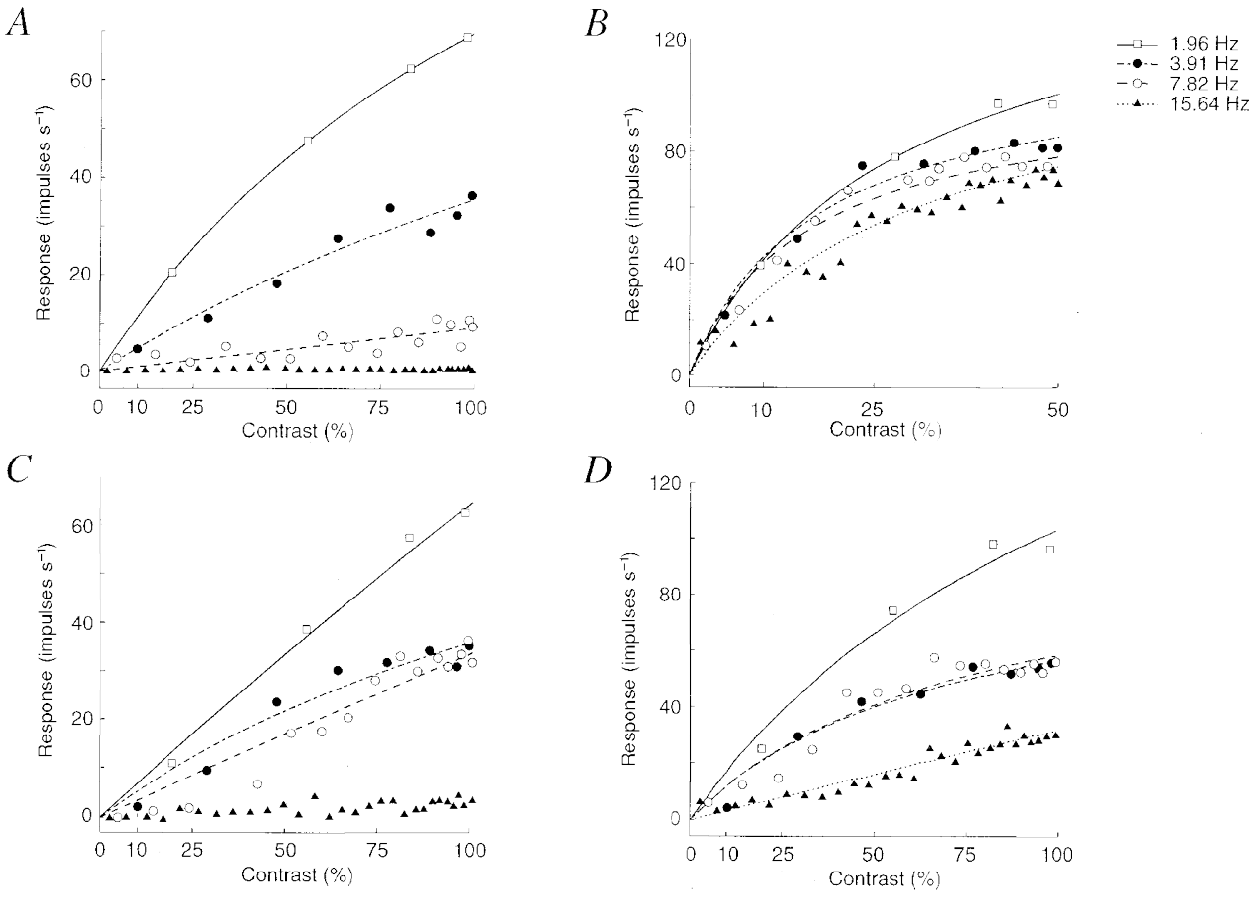

Figure 3. Response amplitude of cells in the marmoset LGN

The response to 4 stimulus frequencies is shown for each cell. *A*, parvocellular cell, 10 deg eccentricity. This cell shows no response saturation at high stimulus contrasts. *B*, magnocellular cell, 3·5 deg. Significant response saturation is present at all frequencies. Note that the maximum stimulus contrast is 50% for this cell. *C* and *D*, koniocellular cells with overlapping receptive fields, recorded within 50 μm of each other. The cell in *C* shows little response saturation and low cut-off frequency. The cell in *D* shows more response saturation and a higher cut-off frequency. The lines show Naka–Rushton functions, as described in the text.

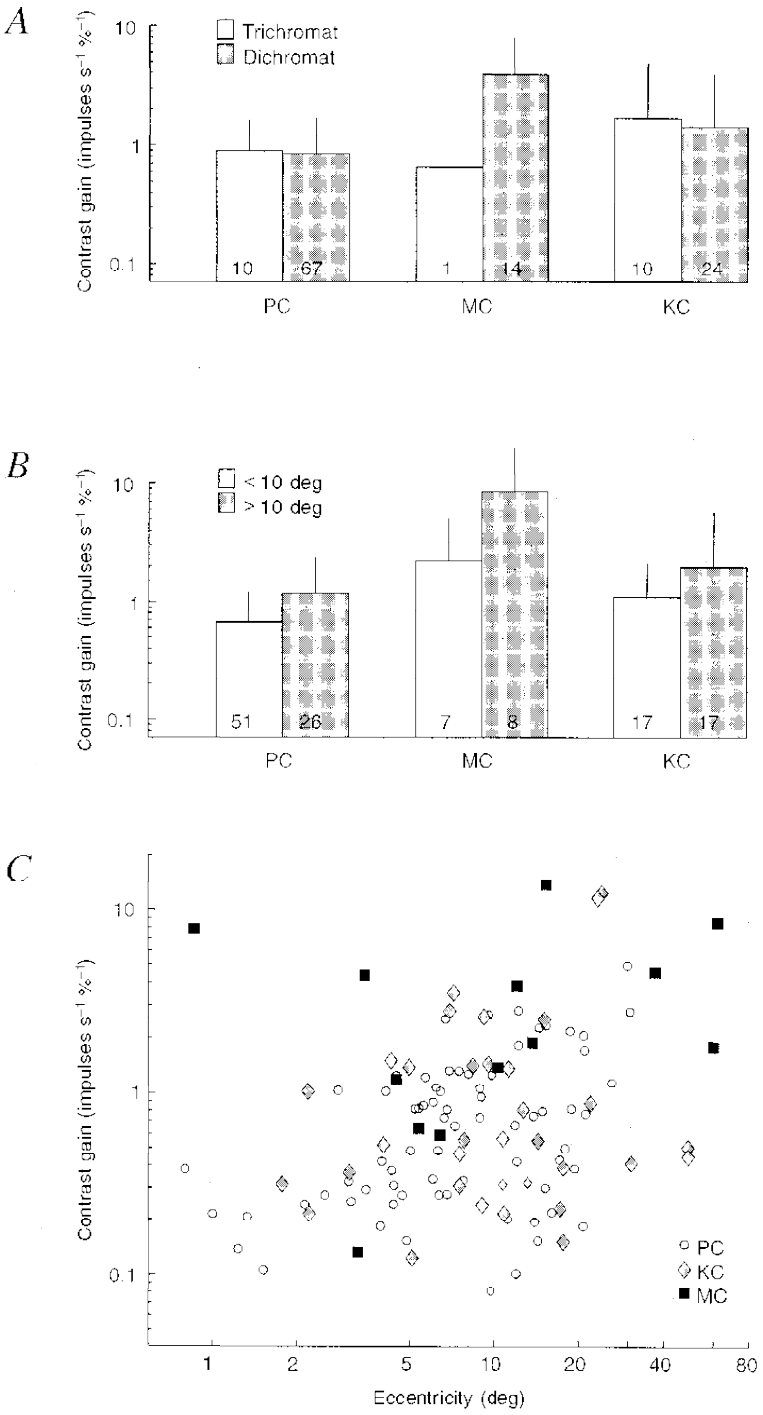

Figure 4. Eccentricity dependence of contrast gain

A, mean contrast gain (+ S.D.) for 3·91 Hz modulation within each LGN subdivision. Comparison of trichromatic and dichromatic marmosets. *B*, comparison of central (below 10 deg eccentricity) and peripheral (above 10 deg eccentricity) receptive field positions. The mean gain of all subdivisions is higher outside the central visual field but does not differ between trichromats and dichromats. *C*, contrast gain for each cell as a function of receptive field eccentricity. PC, parvocellular cell; MC, magnocellular cell; KC, koniocellular cell.

We asked what effect our use of a contrast envelope has on the estimate of contrast gain. For the cell shown in Fig. 2*D*, the gain estimated from the rising phase of the stimulus is 2·18 impulses s^{-1} (% contrast)$^{-1}$, and from the falling phase the estimate is 2·55. This represents an over- or under-estimate of 7·8% compared with the contrast gain measured using the mean values. Applying the same method to the entire cell sample at 3·91 Hz modulation gives a mean discrepancy of 16·5% (S.D. = 17·7%, $n = 52$) for on-centre cells, and 2·8% (S.D. = 13·2%, $n = 68$) for off-centre cells. We have no explanation for the fact than on-centre responses show a greater asymmetry than off-centre responses, but note that these differences are all much smaller than the between-cell variability within each (parvocellular, koniocellular or magnocellular) group (Fig. 4).

Temporal modulation transfer function (TMTF)

We measured contrast sensitivity at five or more temporal frequencies for 42 parvocellular cells, 26 koniocellular cells and 9 magnocellular cells. Examples of TMTFs are shown in Fig. 5. For all groups there is a generalized increase in sensitivity with increasing eccentricity. Of the 77 cells in the sample, 15 responded to a temporal frequency of 31·25 Hz. For the parvocellular group, the proportion of these cells with receptive field eccentricity greater than 10 deg (5/8, 62%) was greater than the corresponding proportion measured at 3·91 Hz (Fig. 4*B*, parvocellular: 26/77, 34%). This difference was not present for the koniocellular or magnocellular groups, but the sample size is small.

In general, magnocellular cells tended to respond to higher temporal frequencies than either koniocellular or parvocellular cells, but there is wide variability in the shape of the TMTFs. There was no clear relationship between the temporal frequency to which the cell was most sensitive and retinal eccentricity (data not shown).

Inspection of the TMTFs (Fig. 5) suggests that the increase in contrast sensitivity in the peripheral retina is more marked at low temporal frequencies. We measured sensitivity to 0·98 Hz modulation in 22 parvocellular and 8 koniocellular cells. Only one magnocellular cell (shown in Fig. 5) responded at this temporal frequency. During the analysis it became apparent that the cells fell into two groups: those from animals where isoflurane was the anaesthetic, and those from animals where sufentanil was used. The sensitivity to 0·98 Hz modulation increases for each group as a function of eccentricity (Fig. 6*A*), but is lower in animals that were anaesthetized with isoflurane. Figure 6*B* shows the relative sensitivity of the cells to moderate (7·80 Hz) and low (0·98 Hz) temporal frequency. This ratio is higher for animals anaesthetized with isoflurane than for animals anaesthetized with sufentanil ($P = 0·0013$, Mann–Whitney U test). In Fig. 7, the TMTFs of parvocellular cells from Fig. 5 (from animals anaesthetized with sufentanil) are superimposed with the TMTFs of parvocellular cells at similar eccentricities from isoflurane-anaesthetized animals. Both these results show that the contrast sensitivity at lower temporal frequencies is decreased by isoflurane.

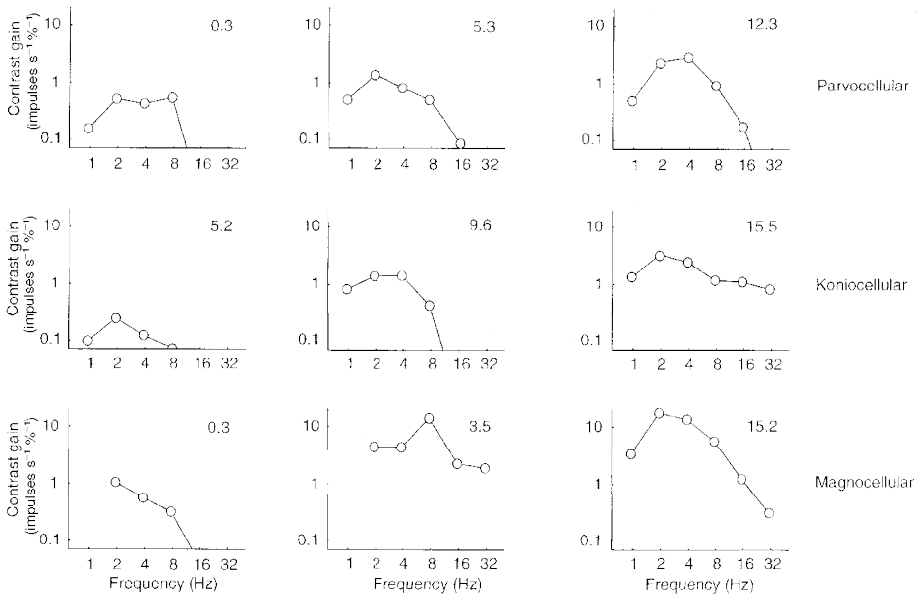

Figure 5. Representative temporal modulation transfer functions (TMTFs)

The receptive field eccentricity (in deg) of each cell is shown at the upper right of each panel. Top row, parvocellular cells. Middle row, koniocellular cells. Bottom row, magnocellular cells. As eccentricity increases, contrast gain increases across temporal frequencies for all cells. The increase in sensitivity is greater for temporal frequencies below 8 Hz.

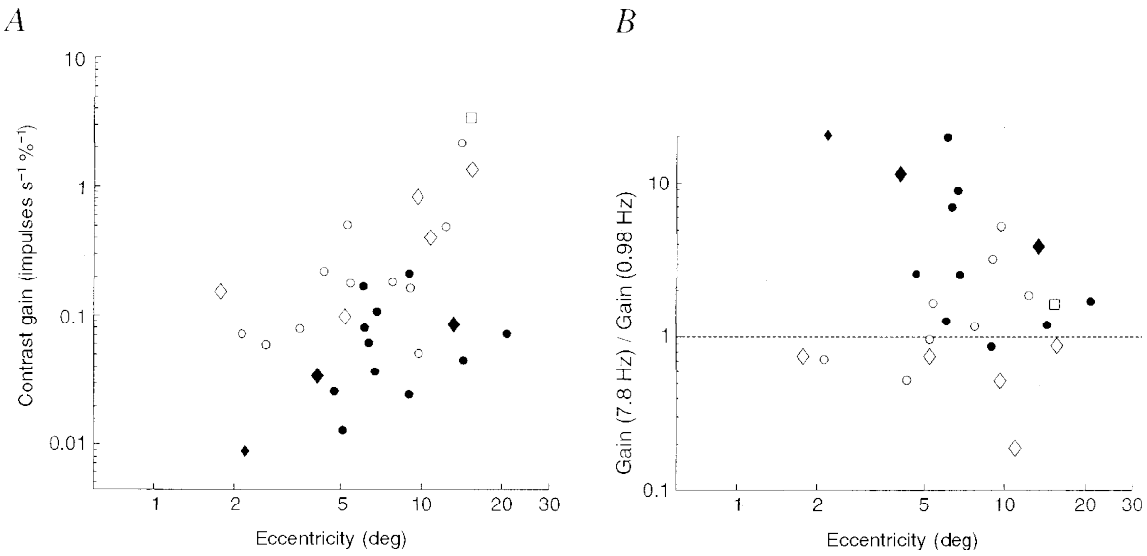

Figure 6. Sensitivity to low temporal frequencies increases with eccentricity and is dependent on the anaesthetic used

A, contrast gain at 0·98 Hz as a function of eccentricity. Gain increases with eccentricity for both parvocellular cells (circles) and koniocellular cells (diamonds). Only one magnocellular cell responded to this stimulus (open square). The sensitivity of cells recorded from isoflurane-anaesthetized animals (filled symbols) is generally lower than that of cells recorded from sufentanil-anaesthetized animals (open symbols). *B*, ratio of sensitivity at 7·82 Hz to sensitivity at 0·98 Hz as a function of eccentricity.

DISCUSSION

We have two main findings. Firstly, within each retinogeniculate pathway, there are eccentricity-dependent changes in contrast sensitivity and temporal transfer properties. Secondly, the temporal contrast sensitivity characteristics of cells in the koniocellular layers of the LGN are intermediate between those of magnocellular and parvocellular cells: koniocellular cells can respond to high flicker frequencies. We now consider the relationship of these results to other properties of, and to the presumed functional roles of, these pathways.

Eccentricity dependence of contrast sensitivity

The contrast sensitivity of magnocellular cells is higher than that of parvocellular cells. This is consistent with results from all primates studied so far (Blakemore & Vital-Durand, 1986; Kaplan & Shapley, 1986; Crook *et al.* 1988; Norton *et al.* 1988; Irvin *et al.* 1993). We also find that the sensitivity to low frequency temporal modulation increases with distance from the fovea (Fig. 3). This effect is strongest for parvocellular cells. The diameter of the stimulus we used (6·4 deg) should encompass both the centre and surround mechanisms of the vast majority of cells. These data can thus be compared with the integrated centre–surround

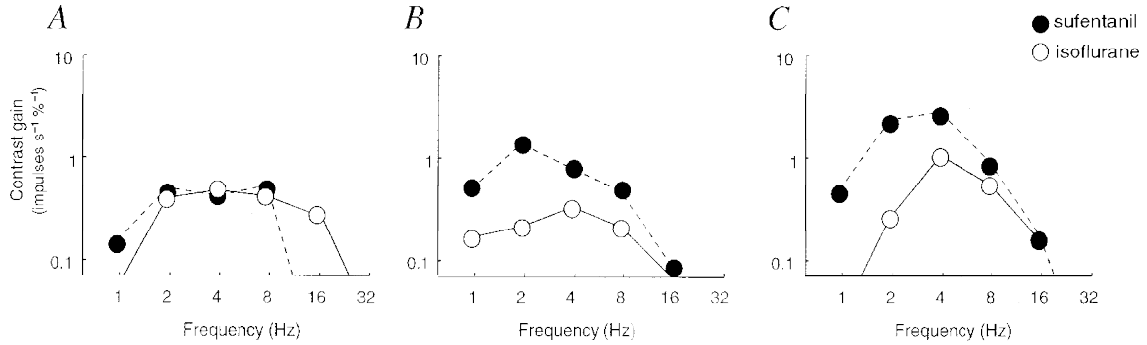

Figure 7. Temporal modulation transfer functions (TMTF) are more low pass in sufentanil-anaesthetized animals

The TMTF of three parvocellular cells (replotted from Fig. 5) from sufentanil-anaesthetized animals are overlaid with the TMTF of three parvocellular cells with similar receptive field eccentricities from animals anaesthetized with isoflurane.

response derived from spatial modulation sensitivity measurements in macaque (Croner & Kaplan, 1995), *Galago* (Irvin *et al.* 1993) and marmoset (Kremers & Weiss, 1997). These studies suggest that the integrated strength or 'volume' (Enroth-Cugell & Robson, 1966) of centre and surround are both relatively independent of receptive field size. This arises because point sensitivity is approximately inversely proportional to diameter, so the sensitivity to diffuse stimuli is rather well matched for cells with different sizes (Derrington & Lennie, 1984; Irvin *et al.* 1993; Croner & Kaplan, 1995). Some variability in the sensitivity to full field stimuli is predicted by this arrangement (Linsenmeier *et al.* 1982; Irvin *et al.* 1993), consistent with the variability seen in Fig. 4. Furthermore, the increase in sensitivity that we see for all cell groups in peripheral visual field is consistent with measurements of centre sensitivity in macaque (Croner & Kaplan, 1995) and marmoset (Kremers & Weiss, 1997; J. Kremers, personal communication) which show that the decrease in point sensitivity is not exactly matched to the increase in area, so there is a slight increase in the integrated strength of the centre for larger centre areas.

Eccentricity-dependent changes in the temporal modulation transfer function

The sensitivity to low frequency (0·98 Hz) modulation increases for parvocellular and koniocellular cells in peripheral retina (Fig. 6*A*). The shape of the TMTF for individual cells (Fig. 5) and the decline in the ratio of sensitivity 7·82 Hz : 0·98 Hz (Fig. 6*B*) show that this is due to reduction in the low temporal frequency rolloff characteristic for individual cells. Assuming that the surround mechanism has a more low-pass temporal characteristic than the centre mechanism (Gouras & Zrenner, 1979; Derrington & Lennie, 1984; Frishman *et al.* 1987; Lee *et al.* 1990), this result also implies that the surround becomes less effective for receptive fields in peripheral retina. Whether increased responsivity to higher temporal frequencies could be explained in the same way is not clear; it could as easily be due to inherent size-dependent changes in the adaptation properties and temporal characteristic of the centre mechanism alone (Enroth-Cugell & Shapley, 1973; De Monasterio & Gouras, 1975; Cleland, 1983). Regardless of these considerations our basic result remains clear: in the peripheral visual field, the sensitivity of many parvocellular and koniocellular pathway cells is at least as great as that of magnocellular cells in central retina.

Anaesthetic-dependent changes in contrast sensitivity

We recorded from LGN cells, and have so far considered their responses as indicative of activity in retinal ganglion cells, but there is convincing evidence for contrast, spatial and temporal-dependent non-linearities in LGN filtering of retinal input (Kaplan *et al.* 1987, 1993; Hamamoto *et al.* 1994; Kremers *et al.* 1997). This is consistent with our finding of anaesthetic-dependent changes in the shape of the TMTF: cells recorded from animals anaesthetized with sufentanil (a μ-opioid agonist) have more low-pass TMTF shapes than those anaesthetized with isoflurane (enflurane). The difference in shape of TMTF that we observe may be due to differential effects on either brainstem or cortical input to the LGN, or activity within the LGN itself (Kaplan *et al.* 1993; Hamamoto *et al.* 1994). Studies in the rat have found that isoflurane anaesthesia and ketamine analgesia have different effects on acetylcholine turnover in different brain regions (Ngai *et al.* 1978). There is a substantial cholinergic input from the brainstem parabrachial region to the LGN of mammals (Mackay-Sim *et al.* 1983; Hutchins & Casagrande, 1988; Eriser *et al.* 1997) that may contribute to the temporal sensitivity differences observed here.

Properties of koniocellular cells

The anatomical and physiological properties of koniocellular pathway cells suggest a distinct contribution to visual processing, but the exact functional role of this pathway remains controversial (for review see Casagrande, 1994). It is now clear that for Old World simians (Livingstone & Hubel, 1982; Hendry & Yoshioka, 1994), Old World prosimians (Lachica & Casagrande, 1992) and New World simian primates (Weber *et al.* 1983; Fitzpatrick *et al.* 1983), cells within the koniocellular layers of the LGN project directly to the cytochrome oxidase-rich 'blobs' in layers 2 and 3 of V1, so their presence as a constant part of the primate geniculostriate pathway is well established.

In the simian primates studied so far, it has been difficult to measure the physiological properties of koniocellular cells, as they are intercalated through the parvocellular and magnocellular layers. In the nocturnal prosimian *Galago*, the koniocellular cells receive input from small, slowly conducting retinal afferents. They have long antidromic activation latency from visual cortex and a large proportion of koniocellular cells show non-concentric receptive field organization (Norton & Casagrande, 1982; Irvin *et al.* 1986, 1993; Norton *et al.* 1988; Lachica & Casagrande, 1993). Many koniocellular cells have a sluggish and transient response to square-wave temporal modulation (Irvin *et al.* 1986).

At first sight there is a discrepancy between these studies and our results, which show that the majority of cells within the koniocellular subdivision of the marmoset have temporal properties intermediate between those of parvocellular and magnocellular cells. The two sets of results are nevertheless compatible. The descriptions of the koniocellular subdivision in *Galago* are based on a multivariate cluster or discriminant analysis, where parameters including conduction latency can be given equal weighting with spatial and temporal parameters (Norton & Casagrande, 1982; Irvin *et al.* 1986, 1993; Norton *et al.* 1988). These studies show indisputably that the koniocellular/interlaminar group is quantitatively distinct from either parvocellular or magnocellular groups. Nevertheless, when any single spatial variable is considered, the spatial properties of many koniocellular cells are intermediate between those of parvocellular and magnocellular cells. The goal of our study was to compare

quantitatively the functional performance of the parvocellular, koniocellular and magnocellular cell groups along a single stimulus dimension, and we arrive at a similar conclusion for the temporal domain as the previous studies do for the spatial domain.

We have not explored quantitatively other response properties of koniocellular cells in marmoset, but our informal measurements of receptive field properties using hand-held stimuli (authors' unpublished observations) and our preliminary quantitative analysis of the spatial properties of koniocellular cells in marmoset (White *et al.* 1999) suggest that our sample may be biased towards koniocellular cells with centre–surround receptive field organization. The cells we encountered which appeared to lack centre–surround organization usually failed to meet the response criterion for measuring sensitivity (see Methods). Norton *et al.* (1988) likewise show that in *Galago*, many or all of the koniocellular cells which lack center–surround organization are very poorly responsive to spatial modulation; also Casagrande (1994, p. 307) emphasizes that the koniocellular cells which do have centre–surround organization show brisk responses to temporal contrast. Our full field stimulus would correspond to low frequency modulation in the spatial domain; a stimulus to which centre–surround-type koniocellular cells in *Galago* are more sensitive than parvocellular cells (Norton *et al.* 1988; Irvin *et al.* 1993). In summary, our results do not argue against the presence of sluggish, poorly responsive cells within the koniocellular division of the retinogeniculate pathway, but we show that, in the temporal domain, many koniocellular cells perform at least as well as parvocellular cells. The extent to which other 'conventional' aspects of visual processing could be subserved by the koniocellular pathway is a matter for further investigation.

Bishop, P. O., Burke, W. & Davis, R. (1962). The interpretation of the extracellular response of lateral geniculate cells. *Journal of Physiology* **162**, 451–472.

Blakemore, C. & Vital-Durand, F. (1986). Organization and post-natal development of the monkey's lateral geniculate nucleus. *Journal of Physiology* **380**, 453–491.

Bonds, A. B., Casagrande, V. A., Norton, T. T. & DeBruyn, E. J. (1987). Visual resolution and sensitivity in a nocturnal primate (galago) measured with visual evoked potentials. *Vision Research* **27**, 845–857.

Casagrande, V. A. (1994). A third parallel visual pathway to primate area V1. *Trends in Neurosciences* **17**, 305–310.

Casagrande, V. A. & Norton, T. T. (1991). Lateral geniculate nucleus: a review of its physiology and function. In *The Neural Basis of Visual Function*, ed. Leventhal, A. G., pp. 41–84. Macmillan Press, Basingstoke, UK.

Cleland, B. G. (1983). Sensitivity to stationary flashing spots of the brisk classes of ganglion cells in the cat retina. *Journal of Physiology* **345**, 15–26.

Croner, L. J. & Kaplan, E. (1995). Receptive fields of P and M ganglion cells across the primate retina. *Vision Research* **35**, 7–24.

Crook, J. M., Lange-Malecki, B., Lee, B. B. & Valberg, A. (1988). Visual resolution of macaque retinal ganglion cells. *Journal of Physiology* **396**, 205–224.

De Monasterio, F. M. & Gouras, P. (1975). Functional properties of ganglion cells of the rhesus monkey retina. *Journal of Physiology* **251**, 167–195.

Derrington, A. M. & Lennie, P. (1984). Spatial and temporal contrast sensitivities of neurones in lateral geniculate nucleus of macaque. *Journal of Physiology* **357**, 219–240.

Enroth-Cugell, C. & Robson, J. (1966). The contrast sensitivity of retinal ganglion cells of the cat. *Journal of Physiology* **187**, 517–552.

Enroth-Cugell, C. & Shapley, R. M. (1973). Flux, not retinal illumination, is what cat retinal ganglion cells really care about. *Journal of Physiology* **233**, 311–326.

Eriser, A., van Horn, S. C. & Sherman, S. M. (1997). Relative numbers of cortical and brainstem inputs to the lateral geniculate nucleus. *Proceedings of the National Academy of Sciences of the USA* **94**, 1517–1520.

Fitzpatrick, D., Itoh, K. & Diamond, I. T. (1983). The laminar organization of the lateral geniculate body and the striate cortex in the squirrel monkey (*Saimiri sciureus*). *Journal of Neuroscience* **3**, 673–702.

Frishman, L. J., Freeman, A. W., Troy, J. B., Schweitzer-Tong, D. E. & Enroth-Cugell, C. (1987). Spatiotemporal frequency responses of cat retinal ganglion cells. *Journal of General Physiology* **89**, 599–628.

Goodchild, A. K. & Martin, P. R. (1998). The distribution of calcium binding proteins in the lateral geniculate nucleus and visual cortex of a New World monkey, the marmoset *Callithrix jacchus*. *Visual Neuroscience* **15**, 625–642.

Gouras, P. & Zrenner, E. (1979). Enhancement of luminance flicker by color-opponent mechanisms. *Science* **205**, 587–589.

Hamamoto, J., Cheng, H., Yoshida, K., Smith, E. L. I. & Chino, Y. M. (1994). Transfer characteristics of lateral geniculate nucleus X-neurons in the cat: effects of temporal frequency. *Experimental Brain Research* **98**, 191–199.

Hendry, S. H. C. & Yoshioka, T. (1994). A neurochemically distinct third channel in the macaque dorsal lateral geniculate nucleus. *Science* **264**, 575–577.

Holdefer, R. N. & Norton, T. T. (1995). Laminar organization of receptive field properties in the dorsal lateral geniculate nucleus of the tree shrew (*Tupaiaglis belangeri*). *Journal of Comparative Neurology* **358**, 401–413.

Hutchins, J. B. & Casagrande, V. A. (1988). Development of acetylcholinesterase activity in the lateral geniculate nucleus. *Journal of Comparative Neurology* **275**, 241–253.

Irvin, G. E., Casagrande, V. A. & Norton, T. T. (1993). Center/surround relationships of magnocellular, parvocellular, and koniocellular relay cells in primate lateral geniculate nucleus. *Visual Neuroscience* **10**, 363–373.

Irvin, G. E., Norton, T. T., Sesma, M. A. & Casagrande, V. A. (1986). W-like response properties of interlaminar zone cells in the lateral geniculate nucleus of a primate (*Galago crassicaudatus*). *Brain Research* **362**, 254–270.

Kaas, J. H., Huerta, M. F., Weber, J. T. & Harting, J. K. (1978). Patterns of retinal terminations and laminar organization of the lateral geniculate nucleus of primates. *Journal of Comparative Neurology* **182**, 517–554.

Kaplan, E., Mukherjee, P. & Shapley, R. (1993). Information filtering in the lateral geniculate nucleus. In *Contrast Sensitivity*, ed. Shapley, R. & Lam, D. M.-K., pp. 183–200. The MIT Press, Cambridge, MA, USA.

Kaplan, E., Purpura, K. & Shapley, R. M. (1987). Contrast affects the transmission of visual information through the mammalian lateral geniculate nucleus. *Journal of Physiology* **391**, 267–288.

Kaplan, E. & Shapley, R. M. (1986). The primate retina contains two types of ganglion cells, with high and low contrast sensitivity. *Proceedings of the National Academy of Sciences of the USA* **83**, 2755–2757.

Kremers, J. & Weiss, S. (1997). Receptive field dimensions of lateral geniculate cells in the common marmoset (*Callithrix jacchus*). *Vision Research* **37**, 2171–2181.

Kremers, J., Weiss, S. & Zrenner, E. (1997). Temporal properties of marmoset lateral geniculate cells. *Vision Research* **37**, 2649–2660.

Lachica, E. A. & Casagrande, V. A. (1992). Direct W-like geniculate projections to the cytochrome oxidase (CO) blobs in primate visual cortex: axon morphology. *Journal of Comparative Neurology* **319**, 141–158.

Lachica, E. A. & Casagrande, V. A. (1993). The morphology of collicular and retinal axons ending on small relay (W-like) cells of the primate lateral geniculate nucleus. *Visual Neuroscience* **10**, 403–418.

Lee, B. B., Pokorny, J., Smith, V. C., Martin, P. R. & Valberg, A. (1990). Luminance and chromatic modulation sensitivity of macaque ganglion cells and human observers. *Journal of the Optical Society of America* A **7**, 2223–2236.

Linsenmeier, R. A., Frishman, L. J., Jakiela, H. G. & Enroth-Cugell, C. (1982). Receptive field properties of X and Y cells in the cat retina derived from contrast sensitivity measurements. *Vision Research* **22**, 1173–1183.

Livingstone, M. & Hubel, D. H. (1982). Thalamic inputs to cytochrome oxidase-rich regions in monkey visual cortex. *Proceedings of the National Academy of Sciences of the USA* **79**, 6098–6101.

Mackay-Sim, A., Sefton, A. J. & Martin, P. R. (1983). Subcortical projections to lateral geniculate and thalamic reticular nuclei in the hooded rat. *Journal of Comparative Neurology* **213**, 24–35.

Martin, P. R., White, A. J. R., Goodchild, A. K., Wilder, H. D. & Sefton, A. E. (1997). Evidence that blue-on cells are part of the third geniculocortical pathway in primates. *European Journal of Neuroscience* **9**, 1536–1541.

Naka, K.-I. & Rushton, W. H. (1966). S-potentials from colour units in the retina of fish (*Cyprinidae*). *Journal of Physiology* **185**, 536–555.

Ngai, S. H., Cheney, D. L. & Finck, A. D. (1978). Acetylcholine concentrations and turnover in rat brain structure during anesthesia with halothane, enflurane, and ketamine. *Anesthesiology* **48**, 4–10.

Norton, T. T. & Casagrande, V. A. (1982). Laminar organization of receptive-field properties in lateral geniculate nucleus of bush baby (*Galago crassicaudatus*). *Journal of Neurophysiology* **47**, 715–741.

Norton, T. T., Casagrande, V. A., Irvin, G. E., Sesma, M. A. & Petry, H. M. (1988). Contrast-sensitivity functions of W-, X-, and Y-like relay cells in the lateral geniculate nucleus of bush baby, *Galago crassicaudatus*. *Journal of Neurophysiology* **59**, 1639–1656.

Smith, V. C., Lee, B. B., Pokorny, J., Martin, P. R. & Valberg, A. (1992). Responses of macaque ganglion cells to the relative phase of heterochromatically modulated lights. *Journal of Physiology* **458**, 191–221.

Solomon, S. G., White, A. J. R., Grünert, U. & Martin, P. R. (1998). Temporal contrast sensitivity of koniocellular cells in the primate visual system. *Society for Neuroscience Abstracts* **24**, 140.

Troilo, D., Howland, H. C. & Judge, S. J. (1993). Visual optics and retinal cone topography in the common marmoset (*Callithrix jacchus*). *Vision Research* **33**, 1301–1310.

Walls, G. L. (1953). *The Lateral Geniculate Nucleus and Visual Histophysiology*. University of California Press, Berkeley, CA, USA.

Weber, J. T., Huerta, M. F., Kaas, J. H. & Harting, J. K. (1983). The projections of the lateral geniculate nucleus of the squirrel monkey: studies of the interlaminar zones and the S layers. *Journal of Comparative Neurology* **213**, 135–145.

Westheimer, G. (1966). The Maxwellian view. *Vision Research* **6**, 669–682.

White, A. J. R., Goodchild, A. K., Wilder, H. D., Sefton, A. E. & Martin, P. R. (1998). Segregation of receptive field properties in the lateral geniculate nucleus of a New-World monkey, the marmoset *Callithrix jacchus*. *Journal of Neurophysiology* **80**, 2063–2076.

White, A. J. R., Solomon, S. G. & Martin, P. R. (1999). Spatial and temporal contrast sensitivity of parallel visual pathways in the common marmoset, *Callithrix Jacchus*. *Proceedings of the Australian Neuroscience Society* **10**, 195.

Wilder, H. D., Grünert, U., Lee, B. B. & Martin, P. R. (1996). Topography of ganglion cells and photoreceptors in the retina of a New World monkey: the marmoset *Callithrix jacchus*. *Visual Neuroscience* **13**, 335–352.

Yeh, T., Lee, B. B., Kremers, J., Cowing, J. A., Hunt, D. M., Martin, P. R. & Troy, J. B. (1995). Visual responses in the lateral geniculate nucleus of dichromatic and trichromatic marmosets (*Callithrix jacchus*). *Journal of Neuroscience* **15**, 7892–7904.

Acknowledgements

We thank Ana Lara for expert technical assistance and Ann Goodchild and Heath Wilder for their participation in some of the recording experiments. We also thank U. Grünert and J. Kremers for helpful comments and discussions. The constructive criticism and comments of the anonymous reviewers is also gratefully acknowledged. We are grateful to ICI Australia for donating the isoflurane used in these experiments. This work was supported by the Australian National Health and Medical Research Council (project grant no. 960970) and the Ramaciotti foundation.

Corresponding author

P. R. Martin: Department of Physiology, F13, University of Sydney, NSW 2006, Australia.

Email: paulm@physiol.usyd.edu.au